Structures and dynamics of glycosphingolipid-containing lipid mixtures as raft models of plasma membrane

2005 J. Phys.: Condens. Matter 17 S2965

(http://iopscience.iop.org/0953-8984/17/31/025)

INSTITUTE OF PHYSICS PUBLISHING JOURNAL OF PHYSICS: CONDENSED MATTER

J. Phys.: Condens. Matter **17** (2005) S2965–S2977 doi:10.1088/0953-8984/17/31/025

Structures and dynamics of glycosphingolipid-containing lipid mixtures as raft models of plasma membrane

M Hirai[1,5], M Koizumi[1], H Hirai[1], T Hayakawa[2], K Yuyama[3,4], N Suzuki[3,4] and K Kasahara[3]

[1] Department of Physics, Gunma University, 4-2 Aramaki, Maebashi 371-8510, Japan
[2] Lipid Biology Laboratory, RIKEN Wako Institute, Saitama 351-0198, Japan
[3] The Tokyo Metropolitan Institute of Medical Science, Tokyo 113-8613, Japan
[4] PRESTO, JST, Japan

E-mail: mhirai@fs.aramaki.gunma-u.ac.jp

Received 28 December 2004
Published 22 July 2005
Online at stacks.iop.org/JPhysCM/17/S2965

Abstract

The structure and function of mammalian plasma membrane microdomains, so-called rafts, are among the hot topics in cell biology, since it is suggested that these domains are involved in important membrane-associated events, especially ones such as signal transduction, which were frequently seen in physiological and immunological studies. In spite of the accumulation of large amounts of evidence, results on physical properties of the structure and dynamics of membranes such as those in intact cells are less abundant. In this report we treat the structure and dynamics of glycosphingolipid (ganglioside)–cholesterol and glycosphingolipid (ganglioside)–cholesterol–phospholipid mixtures used as models of rafts and plasma membranes. The present results clearly show that the incorporation of cholesterol with ganglioside aggregates is limited to a maximum miscibility of the molar ratio between the ganglioside and cholesterol ranging from $\sim 1/1$ to $1/3$ and that small vesicles with diameters of about 250–300 Å form. These molar ratios and sizes agree well with the reported constituent ratio and minimum size for the rafts. In the vesicle systems containing ganglioside, cholesterol, and phospholipid (PC, DSPC, DOPC, POPC), the bending modulus tends to take the smallest value at the molar ratio of [gang]/[chol]/[phospholipid] $= 0.1/0.1/1$. The present results would strongly support a functional physical property of the raft model: sphingolipids and cholesterol clustering to form rafts that move within the fluid lipid bilayer.

(Some figures in this article are in colour only in the electronic version)

[5] Author to whom any correspondence should be addressed.

1. Introduction

Historically, the fluid mosaic model presented by Singer and Nicolson has been used for a long time [1]. They described the plasma membrane as a 'random distribution of membrane proteins in the sea of lipid bilayers'. With the development of brain science and of experimental techniques, especially fluorescence bioimaging and AFM, experimental evidence has been accumulated and has shown the presence of domain aggregates in plasma membranes, especially in neuronal cells. Simon and Ikonen have presented a new concept for the plasma membrane, the so-called raft model [2]. They described a plasma membrane where dynamic clustering of sphingolipids and cholesterol occurs to form rafts that move within a fluid bilayer. Hakomori *et al* has presented another model [3], called the glycosphingolipid (GSL) signalling domain or microdomain model, where they emphasize the important role of GSL clustering in cell signal transduction. The structure and function of mammalian plasma membrane domains, so-called rafts, have been attracting huge interest and are among the current hot topics in cell biology since these domains are assumed to have a significant function as a molecular device for localization of specific proteins and to be involved in important membrane-associated events such as signal transduction, cell adhesion, and lipid/protein sorting [4–6]. A common feature of plasma membrane domains is their peculiar lipid composition: rich in GSLs, sphingomyelin, and cholesterol. Gangliosides are major components of glycosphingolipids. They are acidic lipids composed of a ceramide linked to an oligosaccharide chain containing one or more sialic acid residues (figure 1), which are mostly located on the cell surface membranes and occur richly in the central nervous system. The functionality of the GSLs microdomains is assumed to relate to the peculiar features of GSL molecules both in ceramide and oligosaccharide portions. That is, the sugar head portion of the ganglioside has the ability to form a complex hydrogen bond network. In addition, as a common feature of sphingolipids, this lipid acts as a hydrogen bond acceptor as well as a hydrogen bond donor, whereas glycerolipid acts only as a hydrogen bond acceptor [7]. Therefore, the physiological functions of gangliosides are assumed to be deeply related to such unique features. In spite of the accumulation of great amounts of evidence on the physiological functions of gangliosides, physicochemical studies on the properties of gangliosides and their domain formations are still not abundant, due to the variety of species and to the small amounts of gangliosides in cells. Thus, it is particularly important to elucidate the physicochemical characteristics of ganglioside aggregates since the formation of GSL domains can greatly modify or modulate plasma membrane structures and functions of proteins occluded in membrane, which would relate to the regulation of cell signalling.

Thus, we have been studying physicochemical properties of ganglioside aggregates and the complexes with other lipids by using synchrotron radiation (SR) x-ray and neutron scattering methods. We have clarified several notable characteristics of the aggregated structures in ganglioside micelles and ganglioside-containing vesicles, depending on temperature, pH, salt concentration, and ganglioside molar ratio. We have found evidence for the following. (1) Gangliosides form a prolate ellipsoidal micelle whose sugar chain regions are very hydrophilic. With elevating temperature, hydration and dehydration of sugar chains occur with conformational change of the bending [8–11] and change of the dissociation degree of the sialic acids [12, 13]. These changes accompany thermal hysteresis, depending on the sugar head [14]. (2) In the [G_{M1} ganglioside]/[phospholipid (DPPC)] $= 0.1/1$ system gangliosides predominantly locate in the outer leaflet of the vesicle the same as is assumed in intact plasma membrane [15]. (4) The dehydration and bending of the sugar heads suppress the undulation of the ganglioside micellar structure [16]. (5) In the G_{M1} or G_{D1a} ganglioside–cholesterol system increase of the cholesterol content induces a micelle-to-vesicle transition [17, 18], and there exists a maximum miscibility of cholesterol within G_{M1} gangliosides [18]. The addition of Ca

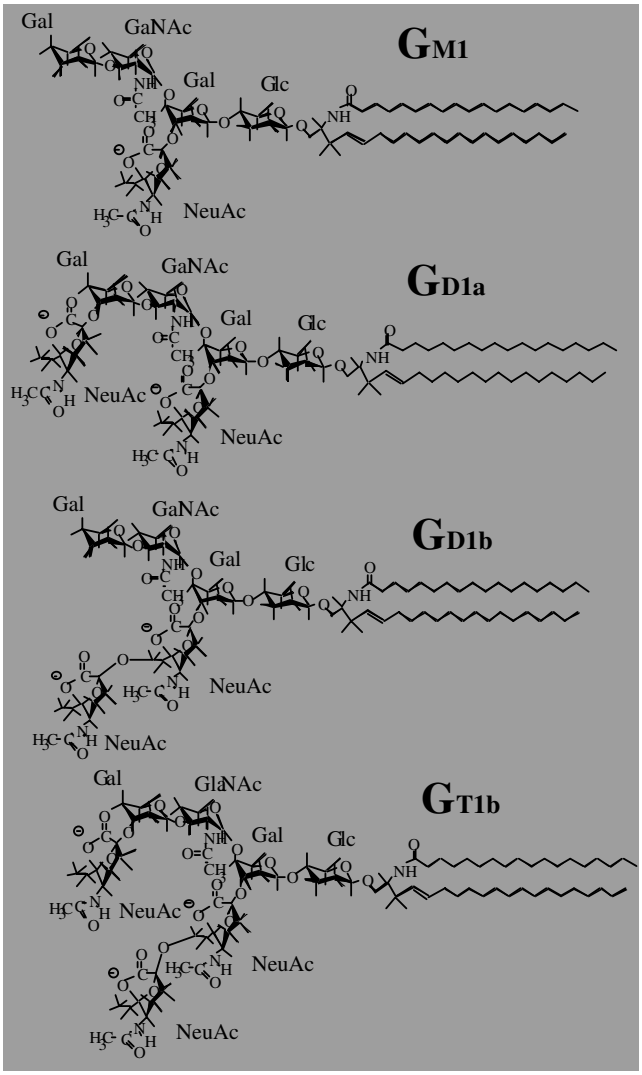

Figure 1. Schematic representation of the molecular structures of G_{M1}, G_{D1a}, G_{D1a}, G_{T1b} gangliosides.

salt induces a vesicle-to-lamellar transition with an interdigitated structure between the sugar heads in the opposing bilayers [18]. These results suggest that the microdomains enriched in gangliosides are able to modulate local charge, hydrophilicity, and dynamics in cell surfaces, which would regulate directly or indirectly the microdomain functions such as accumulation of proteins playing roles in transmembrane signalling events and their activation.

The formation mechanism and the characteristics of GSL microdomains, and their effects on membrane dynamics, are very important for the functions; however, little is known about them. Thus we have carried out further experiments using small angle x-ray scattering (SAXS) and neutron spin echo (NSE) techniques to characterize ganglioside–cholesterol complexes as model raft components and to clarify the dynamics of the model membrane containing ganglioside, cholesterol, and phospholipid.

2. Experimental details

2.1. Sample preparation

The gangliosides used were monosialoganglioside (G_{M1}), disialogangliosides (G_{D1a}, IV^3NeuAc-, II^3NeuAc-GgOse$_4$-Cer; G_{D1b}, II^3NeuAc$_2$-GgOse$_4$-Cer), trisialoganglioside (G_{T1b}, IV^3NeuAc-, II^3NeuAc$_2$-GgOse$_4$-Cer), and type-III (a mixture of G_{M1} and G_{D1}) from bovine brain, purchased from SIGMA Chemical Co. (USA), which were used without further purification. Figure 1 shows the molecular structures of G_{M1}, G_{D1a}, G_{D1b}, G_{T1b} gangliosides. Cholesterol and different types of phospholipid (DSPC, 1,2-distearoyl-*sn*-glycero-3-phosphocholine; DOPC, 1,2-dioleoyl-*sn*-glycero-3-phosphocholine; POPC, 1-palmitoyl-2-oleoyl-*sn*-glycero-3-phosphocholine; PC, L-α-phosphocholine) purchased from SIGMA Chemical Co. and from Avanti Polar Lipids Inc. (USA) were also used without further purification. All other chemicals used were of analytical grade.

For the preparation of ganglioside/cholesterol mixed samples, the required quantities of ganglioside and cholesterol were dissolved in a 2:1 (v/v) mixture of chloroform and methanol. The solvent was removed in a stream of nitrogen gas, and the samples were dried at 45 °C *in vacuo* overnight. The dried samples were suspended in 50 mM HEPES (*N*-(2-hydroxymethyl) piperazine-*N*′-(2-ethane-sulfonic acid)) buffer adjusted to pH 7.0 to become 0.5 wt% ganglioside concentration, and the mixture was stirred for several minutes. For the preparation of the small unilamellar vesicle (SUV) samples of ganglioside/cholesterol/phospholipid mixtures, the required mixtures were also prepared as described above. The dried mixtures were suspended in 50 mM Hepes buffer (pH 7.0), warmed to 45 °C, and stirred at 50 °C for several minutes. The mixtures were sonicated for 10 min at 45 °C by using a high power probe-type ultrasonicator (Model UH-50 of SMT Co.) at 50 W. These sonicated solutions were incubated for 2 h at 45 °C, and kept at 4 °C for ∼12 h before the scattering measurements. For the NSE experiments, the samples were dissolved in D_2O with 50 mM Hepes (pH 7.0). The total lipid concentrations prepared were 0.5% w/v for small angle x-ray scattering (SAXS) and 1% w/v for neutron spin echo (NSE) studies.

2.2. Neutron spin echo and x-ray scattering experiments

NSE experiments were carried out by using an NSE spectrometer [19] installed at the research reactor (JRR-3M) of Japan Atomic Energy Research Institute (JAERI), Tokai, Japan. The sample solutions were contained in a quartz cell controlled at 25 °C. SAXS experiments were carried out by using a SAXS spectrometer installed at the synchrotron radiation source (PF) at the High Energy Accelerator Research Organization (KEK), Tsukuba, Japan. The x-ray wavelength, the sample-to-detector distance, and the exposure time were 1.49 Å, 190 cm, and 300 s, respectively. Other measurement conditions were the same as those for the previous experiments [8–15].

2.3. NSE and SAXS data analyses

The following standard analyses of SAXS data were carried out as reported previously [8–15]. By using the Guinier plot ($\ln I(q)$ versus q^2) for the data sets in the q range from 0.020 to 0.025 Å^{-1}, we determined the values of the radius of gyration R_g by using the following equation:

$$I(q) = I(0)\exp(-q^2 R_g^2/3) \tag{1}$$

where $q = (4\pi/\lambda)\sin(\theta/2)$, and θ and λ are the scattering angle and the x-ray wavelength. The distance distribution function $p(r)$ was obtained by the Fourier transformation of the observed scattering intensity $I(q)$ as

$$p(r) = \frac{1}{2\pi^2}\int_0^\infty rqI(q)\sin(rq)\,\mathrm{d}q. \tag{2}$$

To calculate the function $p(r)$, the extrapolation for the small angle data sets was done by using the Guinier plot, and the modified intensity

$$I'(q) = I(q)\exp(-kq^2) \tag{3}$$

(k is the artificial damping factor) was used to remove the Fourier truncation effect. The maximum diameter $D_{\max}$ of the particles was estimated from the $p(r)$ function satisfying the condition $p(r) = 0$ for $r > D_{\max}$ [20].

The NSE signal amplitude P_{NSE} corresponding to the normalized intermediate correlation function $I(q,t)/I(q,0)$ was obtained from $P_{\mathrm{NSE}} = |A/B|$, where A and B were calculated by applying the following equation to the NSE signal intensity I_{NSE}:

$$I_{\mathrm{NSE}} = A\exp[-a(i-i_0)^2]\cos[b(i-i_0)] + B \tag{4}$$

where i is the symmetry coil current, and a, b, and i_0 are fitting parameters. The NSE signal treatment was described in detail elsewhere [19].

3. Results and discussion

3.1. Micelle-to-vesicle transition and maximum miscibility of cholesterol in gangliosides

Ganglioside and cholesterol are known to be major components of lipid microdomains called rafts [4, 5]. Figure 2 shows the change of the SAXS curve of ganglioside–cholesterol mixtures depending on the cholesterol content, where (A), (B), (C), and (D) correspond to the cases of G_{M1}, G_{D1a}, G_{D1b}, and G_{T1b}, respectively. The molar ratio of ganglioside to cholesterol, [gang]/[chol], was varied from 1/0 to 1/5. The previous model fitting analyses using an ellipsoid structure composed of multi-shells explained reasonably well the observed SAXS curves of the above pure ganglioside solutions ([gang]/[chol] = 1/0) and indicated that these gangliosides are prolate ellipsoidal micelles with the axial ratio of ∼1.3–1.6 in water solvent [8–14]. On increase of the cholesterol content, the scattering curve below $q = 0.05$ Å^{-1} alters from a saturating curve to a steep slope with the change of the profile of the broad hump around $q = 0.1$ Å^{-1}. As shown previously, for the G_{M1}–cholesterol binary mixture [18], the remarkable change of the SAXS curve below $q = 0.05$ Å^{-1} indicates a micelle-to-vesicle transition with the rise of the cholesterol content, which occurs at the molar ratio of [gang]/[chol] = ∼1/2 for G_{D1a}, G_{D1b}, and G_{T1b} in comparison with the case of ∼1/0.4–1/0.6 for G_{M1}.

Figure 3 shows the distance distribution functions $p(r)$ obtained from the Fourier transformation of the scattering curves in figure 2 by using equation (2), where (A), (B), (C), and (D) are as in figure 2. For pure ganglioside samples ([gang]/[chol] = 1/0), every $p(r)$ function is well characterized by the sub-peak or shoulder around $r = \sim$25–28 Å and by the main peak around $r = \sim$71–84 Å. As shown in our previous papers using a shell–ellipsoid modelling analysis [8–14], these distinctive features of the $p(r)$ function are ascribed to the electron density distribution profile of the ganglioside micelle which consists of the hydrophilic sugar head region and the hydrophobic hydrocarbon tail region. The sugar head and tail regions have respectively positive and negative excess average scattering densities, so-called contrasts, against the average scattering density of the solvent. The maximum diameter

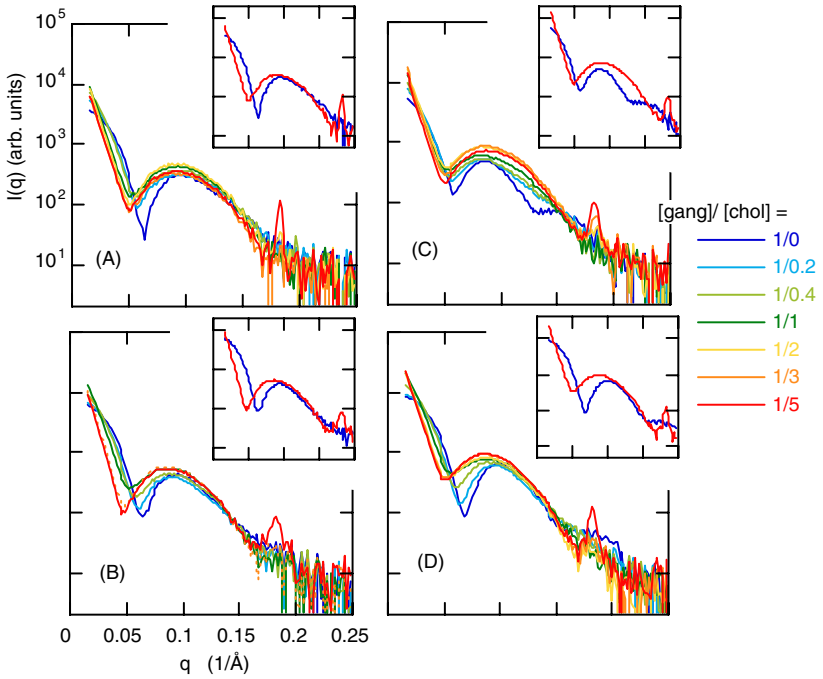

Figure 2. Change of SAXS curve of ganglioside–cholesterol mixtures depending on the cholesterol content, where (A), (B), (C), and (D) correspond to the cases of G_{M1}–cholesterol, G_{D1a}–cholesterol, G_{D1b}–cholesterol, and G_{T1b}–cholesterol mixtures, respectively. The molar ratio of ganglioside to cholesterol, [gang]/[chol], was varied from 1/0 to 1/5.

and the positions of the sub-peak and the main peak for G_{M1} micelle are 127, 26, and 73 Å, respectively, and for G_{D1a}, 124, 26, and 74 Å, respectively. These values agree well with the previous values [8, 9]. On the other hand, these values for G_{D1b} are 144, 25, and 84 Å, respectively, and for G_{T1b}, 113, 28, and 71 Å, respectively. Thus, except for the G_{D1b} case, increase of the number of sialic acid residues tends to create smaller micelles, which could be understood to result from the increase of the surface area suggested in figure 1. The difference between G_{D1a} and G_{D1b} suggests that the binding site of sialic acid also affects the surface area, i.e., the geometrical packing parameter. In all cases in figure 3, with increasing cholesterol content the $p(r)$ function changes continuously and reaches a constant profile above a high cholesterol content, namely [gang]/[chol] $\geqslant \sim 1/1$ for G_{M1}, [gang]/[chol] $\geqslant \sim 1/2$–$1/3$ for G_{D1a}, G_{D1b}, and G_{T1b}. For all species of gangliosides that we studied, the maximum diameters D_{max} of the aggregate structures, estimated from the $p(r)$ functions, take similar values around ∼260–270 Å at high cholesterol contents.

The above tendency is more clearly seen in the dependence of the radius of gyration R_g on the cholesterol content in figure 4 where (A), (B), (C), and (D) are as in figure 2. For all cases in figure 4, with increasing cholesterol content the R_g value begins to increase significantly and becomes saturated. In the G_{M1} case in figure 4(A), the R_g value increases to 89.6 ± 1.2 Å at [gang]/[chol] = 1/1, and above this cholesterol content no major increase was observed. The R_g value at [gang]/[chol] = 1/5 is 92.5 ± 1.3 Å. In the G_{D1a} case in figure 4(B), the R_g value increases significantly to 94.6 ± 2.4 Å at [gang]/[chol] = 1/2 and changes slightly to 97.2 ± 1.2 Å at [gang]/[chol] = 1/5. In the G_{D1b} case in figure 4(C), the R_g value increases from 56.1 ± 0.4 Å (at [gang]/[chol] = 1/0) to 89.3 ± 1.7 Å (at [gang]/[chol] = 1/3) and takes

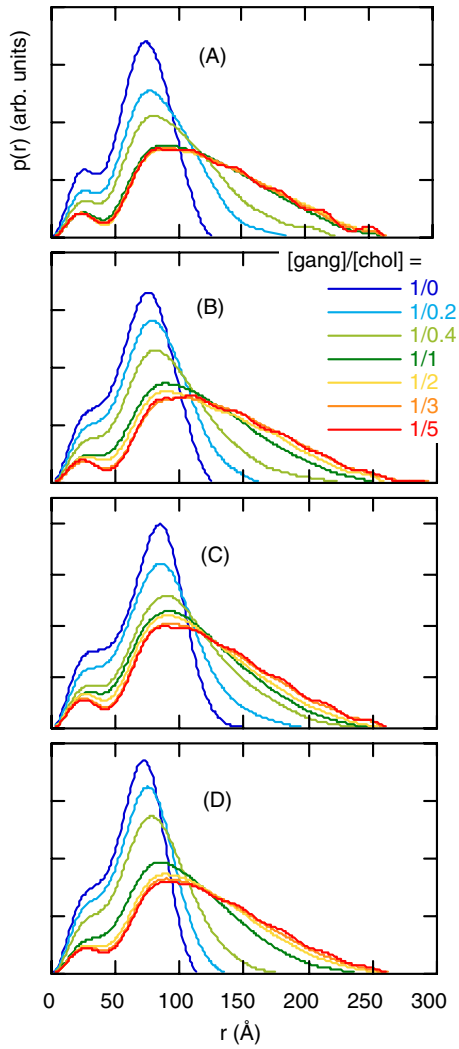

Figure 3. Distance distribution functions $p(r)$ obtained from the Fourier transformation of the scattering curves in figure 2, where (A)–(D) are as in figure 2.

the value 90.9 ± 1.5 Å at [gang][chol] $= 1/5$. In the G_{T1b} case in figure 4(C), the R_g value increases from 44.2 ± 0.8 Å (at [gang]/[chol] $= 1/0$) to 88.2 ± 1.4 Å (at [gang]/[chol] $= 1/3$) and takes the value 90.1 ± 1.7 Å at [gang]/[chol] $= 1/5$. As a common feature for all cases, significant increases of R_g occur in the molar ratio between $1/0$ and $\sim 1/1$.

On the other hand, in figure 2 a reflection peak at $q = \sim 0.18$ Å^{-1} became visible, depending on the cholesterol content. This reflection peak is attributable to the presence of cholesterol monohydrate crystals with periodicity of 34 Å [21]. The molar ratio where the reflection peak appears first agrees with that where the R_g mostly reaches the maximum value first. As shown in figures 2 and 3, the ganglioside–cholesterol mixture takes mostly a constant structure above the molar ratio of [gang]/[chol] $= \sim 1/1$ for G_{M1}, $\sim 1/2$–$1/3$ for G_{D1a}, G_{D1b}, and G_{T1b}. The dynamic light scattering measurements showed that the particles with diameter from 250 to 300 Å occupy around 75% in total number (data not shown), which agrees with the

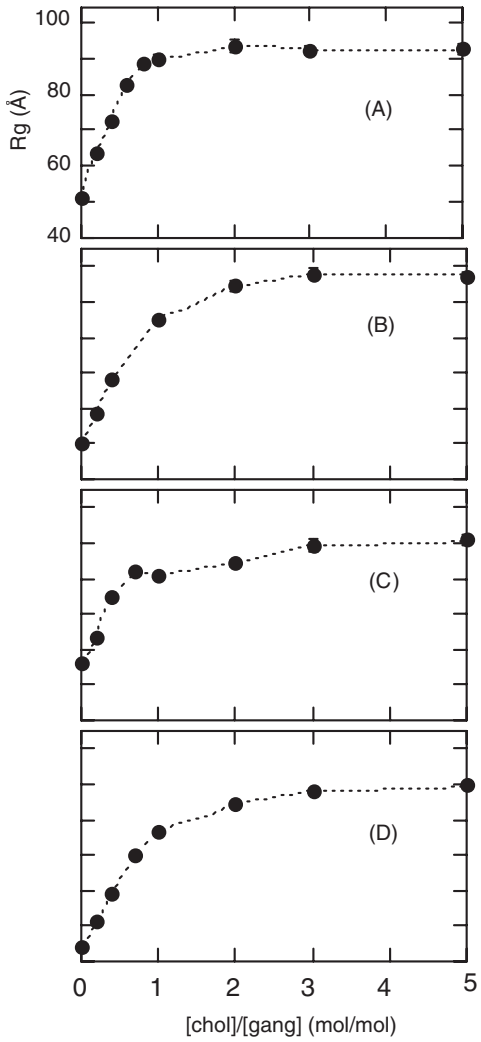

Figure 4. Radius of gyration R_g of ganglioside–cholesterol mixtures depending on the cholesterol content. (A)–(D) are as in figure 2.

D_{max} values estimated from the $p(r)$ functions. According to our previous SAXS results for ganglioside micelles obtained using shell model fitting analyses [8, 9], the length of the head portion of the ganglioside molecule is ∼22 Å and that of the tail portion is ∼26 Å. Therefore, the structure formed is not a multi-lamellar vesicle but a unilamellar one. As demonstrated in our previous SAXS measurements and shell model fitting analyses [17, 18], these indicate the structural transition of the mixture from a micelle to a vesicle via an elongated spherocylindrical micellar structure, which is also suggested by the recent results of EPR measurements [22]. The vesicle structures formed were stable for over one month. Thus, the present results clearly indicate that there exists a miscibility limit for cholesterol in ganglioside aggregate and that ganglioside and cholesterol form a stable and compact vesicle structure with a limited size at the high cholesterol concentration. The maximum miscibility depends on the structure of the head portion of the ganglioside. It should be mentioned that the values determined for

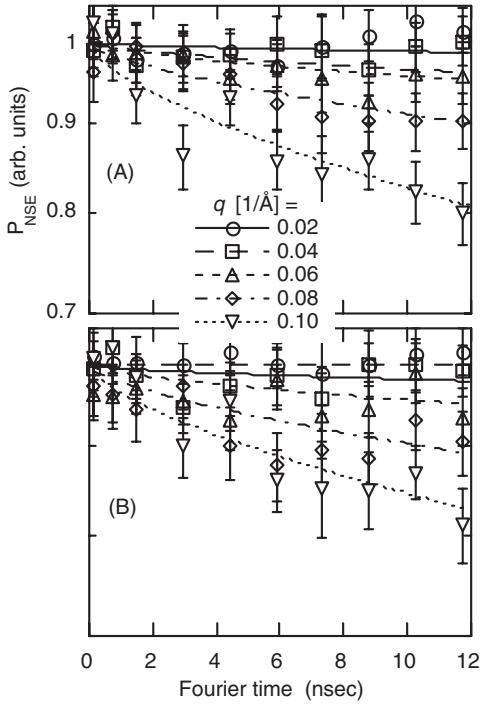

Figure 5. Fourier time dependence of the NSE signal amplitudes P_{NSE} of vesicles at different q values at 25 °C. (A) and (B) correspond to the samples of [ganglioside-type-III]/[chol]/[DOPC] = 0.1/0.1/1 mixture and DOPC alone, respectively. The lines show the fitted results obtained using the stretched exponential $P_{\mathrm{NSE}} = \exp(-(\Gamma t)^{2/3})$.

the maximum miscibility of cholesterol are comparable with the molar ratios of cholesterol to ganglioside in raft fractions reported previously [23, 24].

3.2. Dynamics of the raft model membrane

To clarify the properties of the dynamics of the bilayer membrane as a model of a raft, we carried out NSE experiments for the ternary component lipid systems containing ganglioside, cholesterol, and glycerophospholipid. Figure 5 shows the Fourier time dependence of the NSE signal amplitude P_{NSE} at different q values at 25 °C, which are fitted with a stretched exponential. In figure 5, (A) and (B) correspond to the samples of ganglioside [Type-III]/[chol]/[DOPC] = 0.1/0.1/1 mixture and DOPC alone, respectively. The simple exponential function with the equation $P_{\mathrm{NSE}} = \exp(-\Gamma t)$, which has been ordinarily applied to fluctuating microemulsion droplets to determine the relaxation rate Γ [25, 26], fitted the observed P_{NSE} function poorly. According to the formulation presented by Zilman and Granek [27], we applied the stretched exponential formula to the observed P_{NSE} functions. As shown in figure 5, the P_{NSE} functions are fitted well by the stretched exponential formula, not by the simple exponential. The above stretched exponential formula was introduced theoretically by Zilman and Granek using the Helfrich bending free energy to describe membrane undulations [27]. For the two-dimensional membrane case, Γ was given as follows:

$$\Gamma(q) = 0.025\gamma_\kappa \left(\frac{k_{\mathrm{B}}T}{\kappa}\right)^{1/2} \frac{k_{\mathrm{B}}T}{\eta} q^3 \tag{5}$$

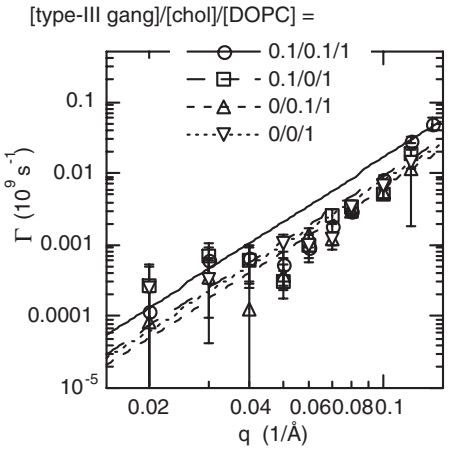

Figure 6. q dependence of the relaxation rate Γ on a log–log scale. The lines show the fitted results obtained using $\Gamma\square = \alpha q^3$ to determine the bending modulus of the membrane.

where κ and η are the bending modulus of the membrane and the viscosity of the surrounding medium, respectively. k_B is the Boltzmann constant. Here $\gamma_\kappa \approx 1$ when $\kappa/k_B \gg 1$. Figure 6 shows the q dependence of Γ on a log–log scale. From the slope depending on equation (5), we estimated the value of the bending modulus κ, where we tentatively used three times the viscosity value of pure D_2O solvent for η at 25 °C, as described in the previous papers [28, 29]. Table 1 summarizes the κ values obtained for the different lipid systems containing ganglioside, cholesterol, and glycerophospholipid. From table 1 we can see several features of the bending modulus, depending on the lipid composition. At the measurement temperature 25 °C, DOPC, POPC, and PC are clearly in the liquid crystalline phase whereas DSPC is in the gel phase [30]. Cholesterol was shown experimentally [31] and theoretically [32] to modify the gel and the liquid crystalline phases differently. The disorder of the gel phase is increased by cholesterol addition, while the liquid crystalline phase is ordered. In table 1 the bending modulus κ for [cholesterol]/DOPC or POPC $= 0/1$ increases on cholesterol addition at $0.1/1$, which is explained by the cholesterol effect on the liquid crystalline phase, whereas the addition of gangliosides seems to simply decrease the κ value for every case. For all ternary systems, the κ values tend to take similar small values at the lipid compositions, as in intact neuronal cells, which are in the range from $\sim 1.1 \times 10^{-20}$ J ($\sim 2.8\, k_B T$) to $\sim 3.7 \times 10^{-20}$ J ($\sim 9.3\, k_B T$). This suggests that at the lipid raft composition the membrane is softened and more fluid, which would strongly support the functionality of the raft model [2]. In comparison with the case for the $[G_{M1}]$/[chol]/DSPC, POPC, and PC systems, the κ values at the $0.1/0.1/1$ molar ratio are mostly of the same order, namely ~ 2.3–2.5×10^{-20} J, suggesting that at the lipid composition of the raft the bending modulus is less sensitive to glycerophospholipid species. On the other hand, the addition of the divalent cation (Ca^{2+}) greatly increases the bending modulus from $\sim 2.5 \times 10^{-20}$ J at $[Ca^{2+}] = 0$ mM to $\sim 8.1 \times 10^{-20}$ J at $[Ca^{2+}] = 10$ mM; that is, the membrane becomes around three times harder, responding sensitively to the presence of Ca^{2+} ions even at low concentration.

We should mention the local viscosity at the interface between the membrane and solvent. According to the NMR measurements [33], the rotational relaxation time of tightly bound water and weakly bound water for ganglioside sugar heads are shown to be 10^{-9}–10^{-8} s and 10^{-11}–10^{-10} s, respectively. The rotational relaxation time of balk water is $\sim 10^{-12}$ s.

Table 1. Values of the bending modulus of the lipid mixed systems containing ganglioside, cholesterol, and glycerophospholipid in D_2O with 50 mM Hepes (pH 7.0) at 25 °C. The total lipid concentrations were 1% w/v for all samples.

Molar fraction G_{M1}	Type-III	Chol	PC	DSPC	DOPC	POPC	POPC	Ca^{2+} conc. (mM)	Bending modulus (10^{-20} J)
0.1		0.1	1					0	2.5 ± 0.5
0.1		0.1	1					3	6.4 ± 0.9
0.1		0.1	1					10	8.1 ± 0.9
0.1		0.1		1				0	2.4 ± 0.8
0.1		0.1				1		0	2.3 ± 0.5
0.1		0				1		0	1.7 ± 0.4
0		0.1				1		0	13 ± 4
0		0				1		0	1.8 ± 0.4
	0.1	0.1			1			0	1.1 ± 0.2
	0.1	0			1			0	3.7 ± 0.7
	0	0.1			1			0	7.7 ± 0.6
	0	0			1			0	5.0 ± 0.5
	0.1	0.1		1				0	3.7 ± 0.1
	0.1	0		1				0	4 ± 1
	0	0.1		1				0	18 ± 4

The reported numbers of the tightly and weakly bound waters per ganglioside molecule are 20–30 and 170–180, respectively. In our previous SAXS studies, by using a precise shell model method [11, 14], we estimated the number of hydrated waters per ganglioside molecule to be ∼130 for GM1 and ∼180 for GD1a and showed their temperature dependence, namely, a thermal dehydration process of the sugar head. These results suggest that the local viscosity of water around ganglioside sugar heads would be higher than that of bulk water. As shown recently [34], the predicted values of local viscosity (effective viscosity) of solvent at the membrane–solvent interface are greatly dependent on the theory. At the present stage, following some published papers [28, 29], we tentatively use three times the value of the viscosity of bulk water. We await further high statistics NSE data and some direct experimental evidence of local viscosity.

4. Conclusion

As described above, we have obtained the following results. Like for the G_{M1}–cholesterol binary system [18], the present SAXS data for the G_{D1a}–cholesterol, G_{D1b}–cholesterol, G_{T1b}–cholesterol binary systems show the existence of a maximum miscibility of cholesterol in the ganglioside aggregate, namely around 2–3 molar ratios of cholesterol to ganglioside (∼1 for the G_{M1}–cholesterol binary system), in the course of a micelle-to-vesicle transition. The concentrations of cholesterol showing the micelle-to-vesicle transition and the maximum miscibility depend on the ganglioside species, which could intrinsically result from the difference in geometrical packing parameters of ganglioside molecules, depending on their huge and bulky sugar head portions. Gangliosides are able to form a stable and compact vesicle with a diameter of about 250–300 Å, in cooperation with cholesterol

at the molar ratio which has a similar extent as in intact raft fraction. From the NSE data on the ganglioside–cholesterol–glycerophospholipid ternary systems, we have found that the bending modulus tends to take its smallest value at the lipid composition of [ganglioside]/[cholesterol]/[glycerophospholipid] $\approx 0.1/0.1/1$, which has a similar extent as in intact neuronal cell including raft. Combining this with the results for the ganglioside–cholesterol binary system, we assume that the preferential interaction between ganglioside and cholesterol induces the formation of ganglioside–cholesterol rich microdomains in the outer leaflet of the membrane, similar to the asymmetric bilayer structure of the ganglioside–glycerophospholipid binary system [15]. As suggested in the fluorescence probe study [35], a preferential interaction between ganglioside and cholesterol might exist due to the intrinsic features in the ceramide moiety of ganglioside with hydroxyl and amide groups and in the hydroxyl group of cholesterol. The formation of ganglioside–cholesterol microdomains would play a role in affording an appropriate fluidity to the membrane and holding a homeostasis of membrane environments, which seems crucially important for the normal transmembrane signalling events such as the accumulation and activation of functional proteins.

We should mention that in the low q region below 0.03 Å^{-1}, the linearity of the relaxation rate Γ is not so good. There would be room left for other possibilities: e.g. that the intermediate structure factor did not follow the single exponential; for example, a higher mode fluctuation cannot be ignored. To clarify the dynamical properties of ganglioside-containing membrane in more detail and quantitatively, we are now executing further NSE measurements to observe more data points with higher statistics over a wide Fourier time range. Interaction between GSL microdomain and proteins evolved in cell–surface signal transductions would be greatly affected not only by change of hydration of the membrane surface [33, 36–38], but also by change of its dynamical features. That is, the structure and dynamics of ganglioside-containing SUVs treated in the present study would suggest an intrinsic role of gangliosides in GSL domain formation and affinity to a given protein in various signal transductions meditated by biomembranes. Unfortunately, the information on the dynamics of GSL membranes is still quite poor; therefore experimental evidence is needed, which may be involved in further development of suitable theoretical models and approaches.

Acknowledgments

We would like to express our grateful acknowledgments to Professors Takeda and Seto, Drs Nagao and Kawabata of the ISSP-NSE instrument group for their help and discussions on the NSE measurements and analyses. This work was performed with the approval of the Photon Factory Programme Advisory Committee of KEK (Proposal Nos 2001G359 & 2003G137) and with the approval of the Neutron Scattering Programme Advisory Committee (NSPAC) (Proposal Nos 00.027, 01.024, 02.007 & 03.189).

References

[1] Singer S J and Nicolson G 1972 *Science* **185** 720
[2] Simons E and Ikonen E 1997 *Nature* **387** 569
[3] Hakomori S *et al* 1998 *Glycobiology* **8** xi
[4] Svennerholm L *et al* 1994 *Biological Function of Gangliosides* (Amsterdam: Elsevier)
[5] Ledeen R W *et al* 1998 *Sphingolipids as Signaling Modulators in The Nervous System* (New York: The New York Academy of Sciences)
[6] Hakomori S 2001 *Trends Glycosci. Glycotechnol.* **13** 219
[7] Pascher I 1976 *Biochem. Biophys. Acta* **455** 433
[8] Hirai M *et al* 1996 *Biophys. J.* **70** 1761

[9] Hirai M *et al* 1996 *J. Phys. Chem.* **100** 11675
[10] Hirai M *et al* 1998 *Thermochim. Acta* **308** 93
[11] Hirai M *et al* 1998 *Biophys. J.* **74** 3010
[12] Hirai M *et al* 1996 *J. Chem. Soc. Faraday Trans.* **92** 4533
[13] Hirai M *et al* 1999 *J. Phys. Chem.* B **103** 10136
[14] Hayakawa T and Hirai M 2002 *Eur. Biophys. J.* **31** 62
[15] Hirai M *et al* 2003 *Biophys. J.* **85** 1600
[16] Hirai M, Iwase H and Hayakawa T 2001 *J. Phys. Soc. Japan* **70** 420
[17] Hayakawa T and Hirai M 2001 *Mol. Cryst. Liq. Cryst.* **367** 631
[18] Hayakawa T and Hirai M 2003 *J. Appl. Crystallogr.* **36** 489
[19] Takeda T *et al* 1995 *Nucl. Instrum. Methods* A **364** 186
[20] Glatter O 1982 *Small Angle X-ray Scattering* ed O Glatter and O Kratky (London: Academic) p 119
[21] Craven B M 1976 *Nature* **260** 272
[22] Pincelli M M, Levstein P R, Fidelio G D and Gennaro A M 2000 *Chem. Phys. Lipids* **104** 193
[23] Ledeen R W and Yu R K 1982 *Methods Enzymol.* **83** 139
[24] Prinetti A, Chigorno V, Tettamanti G and Sonnino S 2000 *J. Biol. Chem.* **275** 11658
[25] Huang J S, Milner S T, Farago B and Richter D 1987 *Phys. Rev.* **59** 2600
[26] Farago B *et al* 1990 *Phys. Rev. Lett.* **65** 3348
[27] Zilman A G and Granek R 1996 *Phys. Rev. Lett.* **77** 4788
[28] Farago B *et al* 1995 *Physica* B **213/214** 712
[29] Takeda T *et al* 1999 *J. Phys. Chem. Solids* **60** 1375
[30] Marsh D 1990 *CRC Handbook of Lipid Bilayers* (Boston, MA: CRC Press)
[31] Vist M R and Davis J H 1990 *Biochemistry* **29** 451
[32] Ipsen J H *et al* 1987 *Biochem. Biophys. Acta* **905** 162
[33] Arnulphi C *et al* 1997 *J. Lipid Res.* **38** 1412
[34] Komura S *et al* 2001 *Phys. Rev.* E **63** 041402
[35] Bagatolli L A, Gratton E and Fidelio G D 1998 *Biophys. J.* **75** 331
[36] Jain M K, Rogers J and DeHaas G H 1988 *Biochim. Biophys. Acta* **940** 51
[37] Maggio B *et al* 1994 *Biophys. Acta* **1190** 137
[38] Daniele J J *et al* 1996 *Eur. J. Biochem.* **239** 105